

Article

Not peer-reviewed version

---

# Elucidation of Expression Patterns and Functional Properties of Archaelhodopsin Derived from *Halorubrum* sp. Ejinoor

---

[Luomeng Chao](#)<sup>\*</sup> and Yuxia Yang

Posted Date: 7 February 2025

doi: 10.20944/preprints202502.0437.v1

Keywords: Halorubrum sp. Ejinoor Archaelhodopsin; light dark adaptation; photochemical reaction cycle; proton pump



Preprints.org is a free multidisciplinary platform providing preprint service that is dedicated to making early versions of research outputs permanently available and citable. Preprints posted at Preprints.org appear in Web of Science, Crossref, Google Scholar, Scilit, Europe PMC.

Copyright: This open access article is published under a Creative Commons CC BY 4.0 license, which permit the free download, distribution, and reuse, provided that the author and preprint are cited in any reuse.

## Article

# Elucidation of Expression Patterns and Functional Properties of Archaeorhodopsin Derived from *Halorubrum* sp. Ejinoor

Luomeng Chao <sup>1,\*</sup> and Yuxia Yang <sup>2</sup>

<sup>1</sup> College of Animal Science and Technology, Inner Mongolia MINZU University, Tongliao, 028000, China

<sup>2</sup> College of Computer Science and Technology, Inner Mongolia MINZU University, Tongliao, 028000, China

\* Correspondence: chaoluomen@126.com

**Simple Summary:** Bacteriorhodopsin (BR) is a light-sensitive protein found in various organisms that converts light into chemical energy. This study focuses on *Halorubrum* sp. Ejinoor Archaeorhodopsin (*HeAR*), a protein similar to BR discovered in a Chinese salt lake. We expressed *HeAR* in *E. coli* and analyzed its properties using various techniques. Our findings show that *HeAR* is purple and adapts to light and dark conditions, with slight differences in its light absorption properties compared to BR. *HeAR* forms trimers and functions as a proton pump, with a photochemical reaction cycle lasting 100 ms. While *HeAR* shares similarities with BR in its reaction intermediates, it exhibits some unique characteristics in the timing and order of these intermediates. These properties suggest that *HeAR* could be a valuable tool in optogenetics, a field that uses light to control cellular activities.

**Abstract:** Bacteriorhodopsin (BR) is a photosensitive membrane protein commonly found in Archaea, bacteria, and eukaryotes. Its biological function involves transferring protons from the cytoplasmic side to the extracellular side, converting light energy into chemical energy through ATP synthesis. Because of its simple structure and stable function, it has been widely studied in the field of optogenetics. The *Halorubrum* sp. Ejinoor Archaeorhodopsin (*HeAR*) was discovered in a salt lake in Inner Mongolia, China, and shares 57% homology with BR. In this study, *HeAR* was expressed in *E. Coli* BL21(DE). Biological function of *HeAR* was analyzed by SDS-PAGE, UV-VIS absorption spectrum, CD spectrum, laser flash photolysis and proton pump activity detection. The results indicated that *HeAR* was purple and demonstrated light-dark adaptation. The maximum absorbance wavelengths for dark-adapted *HeAR*<sup>D</sup> and light-adapted *HeAR*<sup>L</sup> were 550 nm and 560 nm, respectively. The ratio of All-*trans* and 13-*cis* chromophore was 2:1 in *HeAR*<sup>D</sup> and 6:1 in *HeAR*<sup>L</sup>. The CD spectrum showed that *HeAR* also has trimer structure. *HeAR* was also a proton pump and the photochemical reaction cycle was 100 ms. Although there were L, M, N and O intermediates similar to BR in *HeAR*. However, the generation and disappearance time of M state is earlier than that of BR and the M state disappears before the O state. It is likely that other intermediates exist, resulting in a slow cycle. *HeAR*, as a photosensitive tool, may have promising applications in the field of optogenetics.

**Keywords:** *Halorubrum* sp. Ejinoor Archaeorhodopsin; light dark adaptation; photochemical reaction cycle; proton pump

## 1. Introduction

Bacteriorhodopsin (BR) is a light-sensitive membrane protein sourced from the highly salt-loving bacterium *Halobacterium salinarum* (*Hs*)[1]. BR is made up of seven transmembrane  $\alpha$ -helices connected by loops on both the inside and outside of the cell. The chromophore retinal is covalently attached to the amino acid K216 on the seventh  $\alpha$ -helix, forming a Schiff base, and has a molecular weight of 26 kDa[2,3]. BR acts as a light-driven proton pump, synthesizing ATP from a proton gradient to support the growth and development of the bacterium[4]. The abundant expression of BR in *Hs* gives the bacterium its purple color, which is why BR is often referred to as the purple membrane[1]. BR in the *Hs* membrane binds with phospholipids to form a unique trimeric structure,

which can be purified using the sucrose gradient method[5]. The purple membrane has a broad absorption spectrum in the visible region, and upon absorption of a photon, retinal undergoes isomerization, resulting in the formation of several intermediate states K, L, M, N, O before returning to the ground state to complete the photochemical reaction cycle[6]. BR can absorb photons and convert energy, playing a crucial role in the survival and adaptation of the bacterium. Due to its simple structure, functional diversity, and wide range of applications, BR has attracted significant attention. Research indicates that BR has promising applications in biophysical technologies[7,8], the photocatalytic breakdown of organic pollutants, and serves as an essential tool in optogenetics for processing light signals[9–11].

Optogenetics is a research method in cellular biology that merges optics with genetics[12]. Researchers use genetic engineering to introduce light-sensitive proteins into cells, allowing them to activate or inhibit specific cells with light to better understand their functions. Genes that encode light-sensitive proteins are usually transferred to target cells using methods like transfection, viral transduction, or by creating transgenic animals, which help regulate light signals and observe cellular behaviors and functions[13]. Due to its many advantages such as non-invasive, high spatial and temporal resolution, quantitative repeatability, and simplicity of use, optogenetics has gained widespread attention in neuroscience, molecular biology, and medicine[14–16]. Commonly used light-sensitive proteins in optogenetics research include Channelrhodopsin-2 (ChR2) from the green alga *Chlamydomonas Reinhardtii* and halorhodopsin (*NpHR*) from the halophilic archaeon *Natronomonas Pharaonis*[17,18]. ChR2 has an absorption wavelength range of 350-550 nm with a peak absorption wavelength of 470 nm, while NpHR has an absorption wavelength range of 525-620 nm with a peak absorption wavelength of 578 nm, indicating different sensitivities to light of different wavelengths between the two proteins. Light at 470 nm and 578 nm does not penetrate tissues well, making it challenging to directly activate light-sensitive proteins in deeper cells. To address this problem, researchers discovered a light-sensitive protein from the primitive green alga *Mesostigma viride*, which has a maximum absorption wavelength of 530 nm[19]. Additionally, genetic modifications have been made to VChR1 (Channelrhodopsin from *Volvox carteri*) to produce a light-sensitive protein with an absorption wavelength in the range of 590-630 nm[20]. Apart from ChR2 and NpHR, the most commonly used BR class protein, Archaelhodopsin-T, which can be activated by red light, pumps protons from the inside to the outside of cells, hyperpolarizes the cell membrane, and inhibits cell excitability[20]. Due to the unique biological functions of bacterial rhodopsin proteins, they play an important role in the field of optogenetics. However, as important tools in optogenetics, the search for light-sensitive proteins that meet the requirements and are highly efficient is crucial[21,22].

This study focuses on the *Halorubrum* sp. Ejinoor sensory rhodopsin protein (*HeAR*). *HeAR* was discovered in halophilic bacteria from a salt lake in Inner Mongolia. It has 57% homology to bacteriorhodopsin (BR), features seven transmembrane  $\alpha$ -helical regions, and contains highly conserved amino acids associated with proton pumping (Figure 1). *HeAR* was expressed in the *E. coli* BL21 (DE) expression system prior to the analysis of its biological functions. The biological functions of *HeAR* were analyzed using SDS-PAGE, UV-visible absorption spectroscopy, CD spectroscopy, laser flash photolysis, and proton pump activity assays.

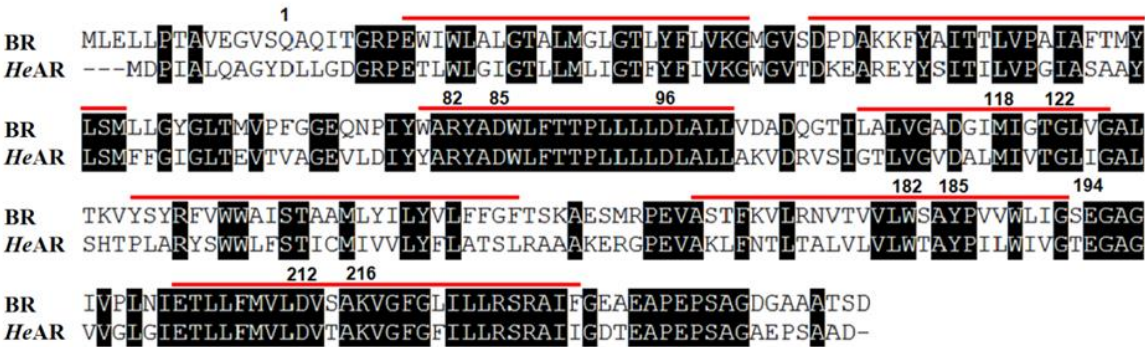


**Figure 1.** Comparative amino acid sequence Alignment between Bacteriorhodopsin and *HeAR*. Proton transport amino acids with numbering and helical segment (uplined) for Bacteriorhodopsin.

2. Materials and Methods

2.1. Expression and Purification of Bacteriorhodopsin Proteins

The nucleic acid genome was extracted from *Halorubrum* sp. ejinoor. PCR amplification was then performed using *HeAR*-specific primers. The PCR product was separated by agarose gel electrophoresis and cloned into the pT7blue plasmid. The obtained DNA sequence was analyzed using an ABI3130/3130xl genetic analyzer[23]. The *HeAR* gene was digested with *NdeI*/*XhoI* enzymes and inserted into the pET21c(+) plasmid to express *HeAR*. This insertion strategy resulted in an additional 8 amino acids (LEHHHHHH) at the C-terminus, providing convenience for subsequent purification. The inserted gene sequence was confirmed by sequencing again using an ABI3130/3130xl genetic analyzer. The recombinant plasmid was then transformed into *Escherichia coli* BL21 (DE3) strain for expression[24].

In LB medium containing 50 µg/mL kanamycin, *Escherichia coli* BL21 (DE3) was cultured at 37 °C, 180 rpm/min until the OD600 of bacterial exponential growth phase reached 0.6. To induce the target protein, 1 mM isopropyl β-D-1-thiogalactopyranoside (IPTG) and 10 µM All-*trans* retinal were added[25]. After induction for 8 hours, cells were harvested by centrifugation at 6000 g for 30 min. The cell pellet was then lysed and membrane proteins were solubilized in buffer containing 1.5% n-dodecyl-β-D-maltopyranoside (DDM) as a detergent[26]. Purification of *HeAR* and BR was further carried out using Ni-NTA agarose chromatography to separate the membrane protein from *Hs*[27]. *Hs* was cultured in *halobacterial* medium and BR was purified by sucrose density gradient ultracentrifugation. The purified *HeAR* and BR were subjected to biological characterization.

2.2. Absorption Spectra and CD Spectra in Light Adaptation State

*HeAR* and BR were dissolved in a 10 mM HEPES buffer (4-(2-Hydroxyethyl)-1-piperazineethanesulfonic acid, pH 7.5) containing 0.05% DDM and were left at room temperature overnight to create dark-adapted samples, *HeAR*<sup>D</sup> and *BR*<sup>D</sup>[28]. After illuminating the *HeAR*<sup>D</sup> and *BR*<sup>D</sup> solutions with 500 nm light to obtain the light-adapted samples, *HeAR*<sup>L</sup> and *BR*<sup>L</sup>, the absorption spectra of both light- and dark-adapted samples were measured using an MPS2000 UV-visible spectrophotometer. Circular dichroism (CD) spectra of *HeAR* and BR were recorded in a solution containing 0.15% DDM and 10 mM HEPES (pH 7.5) using a JASCO J-1500 CD spectrometer.

2.3. Analysis by High Performance Liquid Chromatography of Isomeric Yellow Dye

The extraction method for the retinylidene photoreceptor and bacteriorhodopsin (*HeAR* and BR) followed the protocol established by Dai et al. [29]. The isomeric content of retinylidene chromophores in both light and dark-adapted states was analyzed using high-performance liquid chromatography with a JASCO FLC-350. A total of 100 µL of *HeAR* and BR (0.15% DDM, 10 mM HEPES, pH 7.5) was extracted. Then, 100 µL of hydroxylamine and 300 µL of methanol were added

and mixed thoroughly, followed by the addition of 600  $\mu\text{L}$  of hexane. After centrifugation, the supernatant was collected, and the organic solvent was dried under nitrogen. Finally, 50  $\mu\text{L}$  of hexane was added for high-performance liquid chromatography detection.

#### 2.4. Photochemical Reaction Cycle and Proton Pump Function Detection

Light-induced absorbance changes were measured using an ND-YAG laser (532 nm, 7 ns) flash photolysis setup [30]. Absorbance changes were measured at 10 nm intervals across the visible range (320-700 nm). The flash photolysis data analysis referenced the model developed by Dai et al. [29]. All samples were prepared in a solution containing 10 mM HEPES, 100 mM NaCl, 0.05% DDM, pH 7.5, with an optical density (OD<sub>560</sub>) of 0.7. *Escherichia coli* BL21 (DE3) expressing HeAR was dissolved in a 1M NaCl solution, and changes in H<sup>+</sup> concentration were detected using a pH-sensitive detector after exposure to intense light [31].

### 3. Results

#### 3.1. Induction Expression and Purification of Photosensitive Proteins

The HeAR gene was cloned into the pET21c(+) vector and transformed into *E. coli* BL21(DE3) for protein expression. Following an 8-hour induction with IPTG, the bacterial culture transitioned from pale yellow to a deep purple-red. The purified HeAR and BR proteins exhibited a purple color (Figure 2a), indicating that bacteria with active proton pumps might appear purple because of these proteins. SDS-PAGE analysis of HeAR and BR showed distinct bands at approximately 27 kDa (Figure 2b). This finding aligns with the predicted molecular weights derived from the amino acid sequences of both proteins cloned into the vector, confirming successful purification.

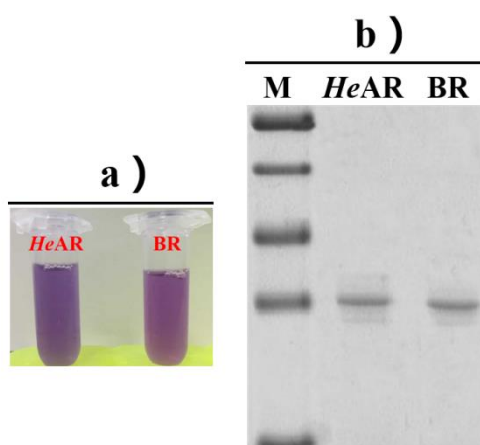


**Figure 2.** Microbial rhodopsins: BR and HeAR. (a) Comparison of the color of the HeAR and BR. (b) The expression of the HeAR and BR analyzed by SDS-PAGE.

#### 3.2. Detection of the Secondary Structure of Photoactive Proteins

BR interacts with phospholipids and retinal to form a unique structure as a trimer, which can be detected by CD spectroscopy. At pH 7.5 (50 mM HEPES, 0.05% DDM), the CD spectrum of HeAR resembles that of BR. However, its maximum absorption wavelength is red-shifted by 10 nm compared to BR. In the CD spectra, HeAR and BR exhibit positive peaks at 525 nm and 535 nm, while negative peaks are observed at 567 nm and 577 nm (Figure 3). These observations suggest that HeAR has a unique trimeric structure that is similar to that of BR.

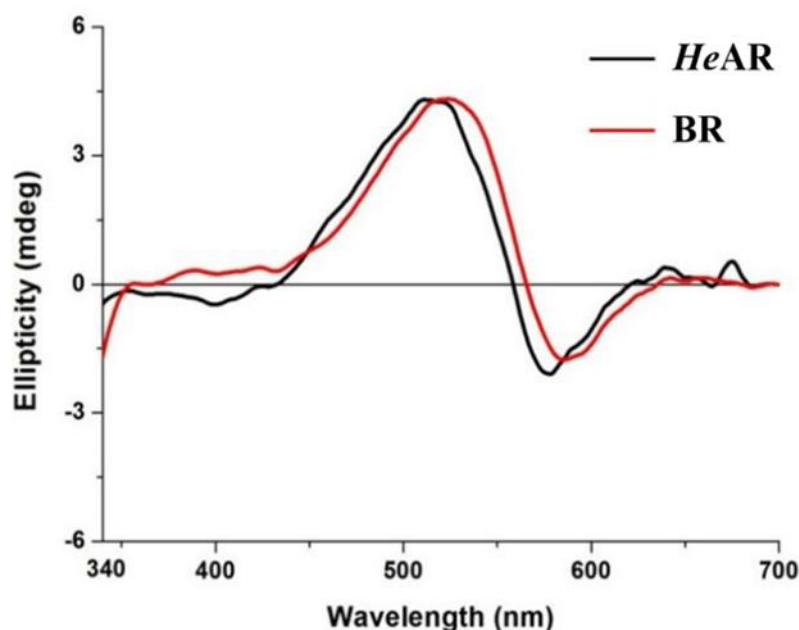


**Figure 3.** The CD spectra of HeAR and BR.

### 3.3. Light and Dark Adaptation States and Composition of Visual Arrestin Isoforms

Bacteriorhodopsin (BR) interacts with the retinal chromophore in its binding region, allowing it to absorb a wide range of wavelengths in the visible spectrum and to exhibit both light and dark adaptation states, with maximum absorption peak wavelengths ( $\lambda_{\text{max}}$ ) of 568 nm for light adaptation and 558 nm for dark adaptation. In darkness, both the *All-trans* and *13-cis* forms of retinal coexist. When illuminated, the *13-cis* retinal chromophore converts to the *All-trans* form, leading to the light-adapted state. If the light-adapted protein is placed in darkness, it reverts to the dark-adapted state. HeAR also shows light and dark adaptation states. The transformation from HeAR<sup>L</sup> with a maximum absorption of 550 nm to HeAR<sup>L</sup> with a maximum absorption of 560 nm takes 2560 seconds (Figure 4a). The transition from BR<sup>D</sup> ( $\lambda_{\text{max}}$  568) to BR<sup>L</sup> ( $\lambda_{\text{max}}$  578 nm) requires 320 s, with a 10 nm blue shift in both cases (Figure 4c). Figure 4b shows that HeAR<sup>L</sup> changes to HeAR<sup>D</sup> after about 160 minutes in the dark, whereas BR<sup>L</sup> converts to BR<sup>D</sup> in 80 minutes (Figure 4d). Variations in the composition of retinal chromophore isomers in proteins can cause changes in their absorption spectrum maximum values. To determine the isomeric composition of retinal chromophores in both light and dark adaptation states of HeAR, we analyzed the extracted retinal chromophores using high-performance liquid chromatography (HPLC). Retinal chromophores exhibit a strong absorption peak at 350 nm, allowing us to calculate their content ratios from the peak values. HPLC analysis showed that both HeAR and BR contain only two retinal chromophore isomers: *All-trans* and *13-cis*. The calculated ratios of retinal isomers are as follows: HeAR<sup>D</sup> has a ratio of *All-trans* to *13-cis* of 2:1, HeAR<sup>L</sup> has 6:1, BR<sup>D</sup> has 1:1, and BR<sup>L</sup> has 6:1 (Figure 5). The results obtained for BR are consistent with those reported by Maeda et al. [32] previously. This indicates that during the transformation of HeAR from light to dark adaptation states, as the content of *13-cis* retinal chromophore decreases, the content of *All-trans* retinal chromophore gradually increases. It is possible that during the photochemical cycle reaction, the isomeric composition of retinal chromophores undergoes changes from *All-trans* to *13-cis* and back to *All-trans*.

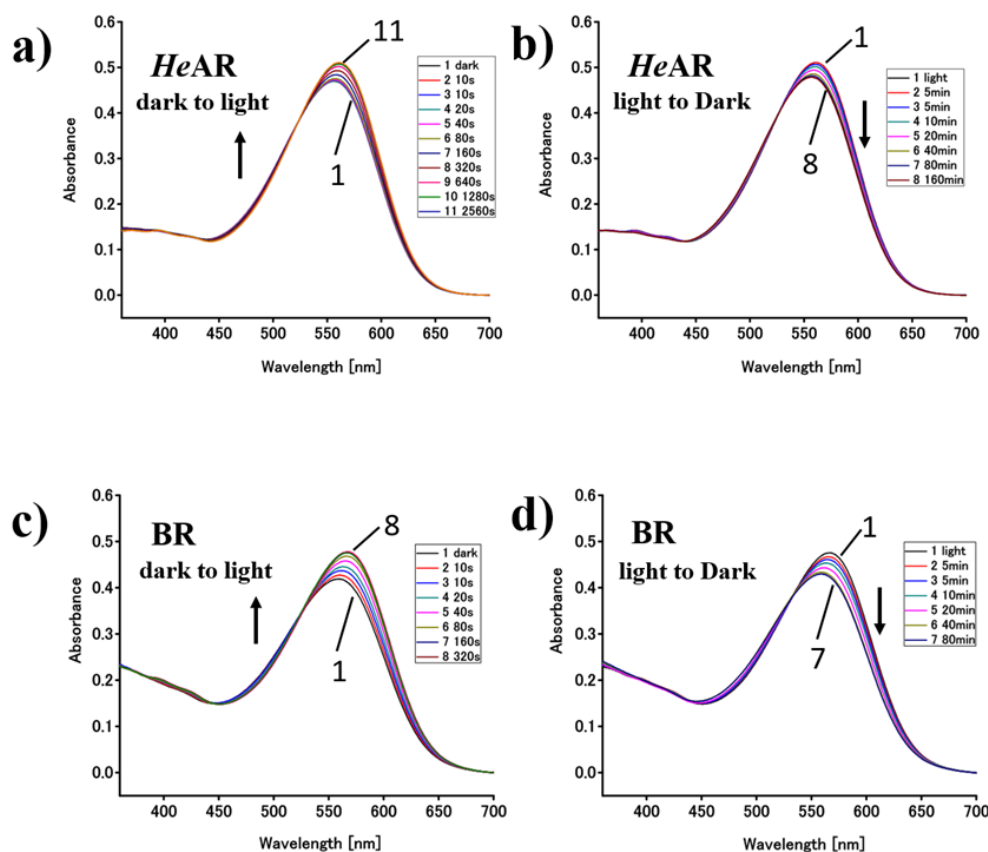


**Figure 4.** Comparison of the light-dark adaptation of purified *HeAR* and *BR* suspended in 10 mM HEPES, pH 7.5 at 20 °C. Light adaptation of purified *HeAR* (A) and *BR* (B). Curve 1 in A and B: *HeAR* (dark) and *BR* (dark). Curves 2-11 in A and B: products of the successive irradiation of *HeAR* (dark) (A) and *BR* (dark) (B) at 500 nm for 10, 10, 20, 40, 80, 160, 320, 640, 1280, and 2560 s, respectively. Dark adaptation of *HeAR* (C) and *BR* (D). Curve 1 in C and D: the curve 11 in *AR* (A) and curve 9 in *BR* (B), respectively. Curves 2-9 in C and D: products of the successive dark incubation of the mixture. The spectra were measured at 5, 5, 10, 20, 40, 80, 160, and 320 min from the beginning of the dark incubation, respectively.

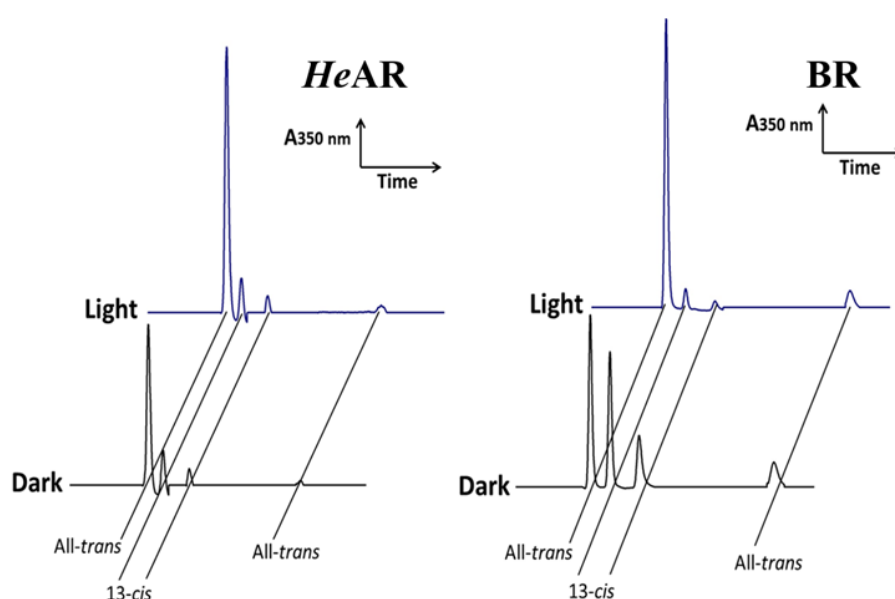


**Figure 5.** Retinal isomer comparison of light-dark adapted pigment by HPLC analysis. The terms “Dark” and “Light” in the panels indicate those obtained using dark and light adapted samples, respectively.

### 3.4. Photosensitive Protein Photochemical Reaction Cycle and Proton Pump

After absorbing light, BR undergoes a photoreaction cycle. Upon light exposure, BR rapidly forms various structural intermediates. Each intermediate has unique maximum absorption peaks. In this study, using BR as a model, the time-dependent absorption wavelength changes of intermediates representing different states, namely M (410 nm), L/N (540 nm), O (670 nm), and the ground state (570 nm), were analyzed. As shown in Figure 6, *HeAR* also exhibits L, M, and O intermediates similar to BR, which change rapidly over a very short period, transitioning between states before returning to the ground state. Initially, the signals for both the *HeAR* ground state and L state decrease at 60  $\mu$ s, while the M state signal increases and reaches saturation at the same time. Subsequently, as the M state signal weakens, a faint O state signal increases, with the M state signal disappearing completely at 3.3 ms, taking a total of 100 ms for all intermediates to vanish. Similarly for BR, the L state and ground state signals decrease (0.3 ms), while the M state signal increases, reaching saturation at 0.2 ms. Shortly after, the M state signal decreases while the O state signal increases, followed by a return to the ground state, completing the entire cycle in about 11 ms. These results indicate that *HeAR* also undergoes a photoreaction cycle, but with a longer duration compared to BR. Notably, the generation and disappearance times of the M state in *HeAR* are quicker than in BR, as the M state disappears before the O state does in *HeAR*. In contrast, in BR, the M state and O state return to the ground state together. This suggests that *HeAR* may involve additional intermediates that contribute to the slow cycling process.

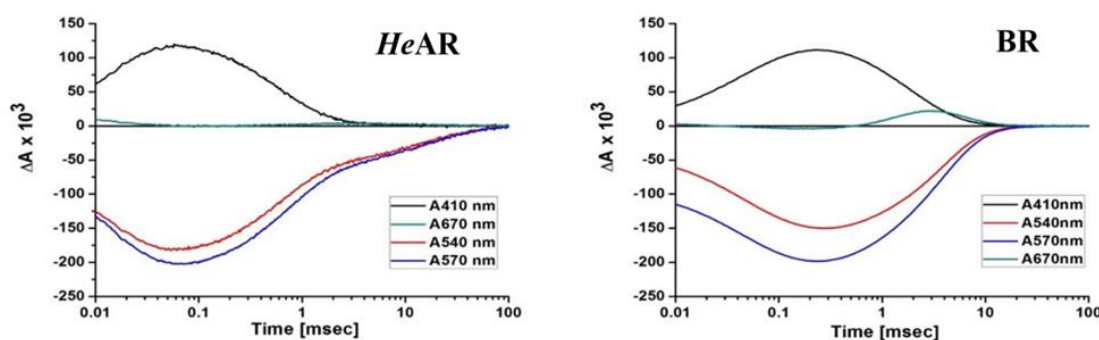


**Figure 6.** Comparison of the flash-induced absorbance changes of the *HeAR* and BR. Samples were measured at four wavelengths: 410, 540, 570, and 670 nm.

We tested the proton pump activity in *E. coli* that expressed the *HeAR* gene. Visual observation showed an increase in H<sup>+</sup> concentration in the bacterial solution upon illumination (Figure 7). This suggests that, like BR, *HeAR* also possesses the ability to transport protons outward. Proton pump activity is a crucial factor in achieving light-controlled target cell modulation, as it can induce membrane hyperpolarization and inhibit cell excitability. Currently, light-driven proton pumps, such as Archaelhodopsin-T, are used to efficiently optogenetically silence neuron cells. Under yellow light activation, proton-pumping proteins move positively charged protons from inside neurons to the external environment. This process leads to hyperpolarization, which helps maintain neuron stability. When the yellow light is turned off, Archaelhodopsin-T rapidly closes ion transport channels compared to NpHR, enabling quick light control over neuron cells at low light power. Therefore, light-driven proton pumps are considered highly efficient tools for optogenetic applications. *HeAR*, as a proton transporter, may also serve as an excellent photosensitive tool for optically inhibiting neuron cells.

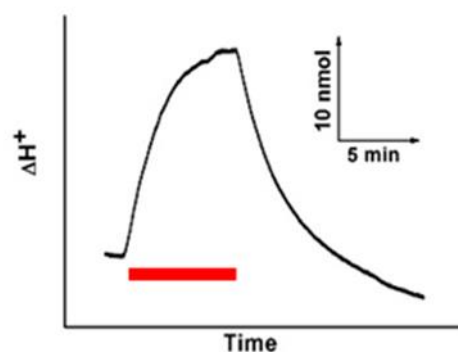


**Figure 7.** Light-induced ion movement of the *E. coli* cell expressing HeAR. The red bar indicates the period of illumination by orange light ( $590 \pm 8.5$  nm). A, Pump activity of HeAR expressing *E. coli* cell suspensions in 50 mM HEPES, 1M NaCl, pH 7.5.

#### 4. Discussion

HeAR was successfully expressed and purified using *E. coli* BL21 (DE3) and, similar to BR, appeared purple. It is likely that the color of proton pump-active bacterial rhodopsin proteins is also purple. These photosensitive proteins could serve as biochemical staining tracers. The unique biological characteristics of bacterial rhodopsin proteins include light adaptation and the photocycle process [33]. The retinal in the protein forms a covalent bond with surrounding amino acids, and the photocycle is completed as the retinal structure changes with light exposure. Studies have shown that one photocycle releases one proton [34]. Therefore, the composition of retinal isomers to a large extent affects the biological function of the protein. Like BR, HeAR has two isomeric forms of retinal in the dark-adapted state: All-*trans* and 13-*cis*, with a ratio of 2:1, whereas BR has a 1:1 ratio. After light exposure, most of the 13-*cis* form of HeAR converts to the All-*trans* form, entering the light-adapted state. In the light-adapted state, HeAR undergoes the photocycle when excited by light, with retinal isomerization cycling through All-*trans*, 13-*cis*, and back to All-*trans*, followed by several intermediate states before returning to the ground state. Our study shows that HeAR also has M, L, and O states similar to BR, but the entire cycle is 90 mS slower than BR. Although HeAR also exhibits proton pump activity, its efficiency may be lower than that of BR based on the logic of one proton released per photocycle. Unfortunately, BR cannot be expressed in other tissue cells, making it unsuitable for optogenetics. The homology between Archaeorhodopsin-T and HeAR is 95%, indicating that HeAR may also have certain value in optogenetic research. This research focuses on expressing and purifying HeAR in bacteria. Additionally, it aims to detect the protein's photosensitive activity and explore its characteristics. Future research will shift towards expressing HeAR in animal models, particularly in mice, to verify its application value in optogenetic studies. This approach will enhance our ability to assess the potential of HeAR in regulating neural activity and understanding neural circuits, ultimately providing new tools and insights for the research and treatment of related diseases.

#### 5. Conclusions

This study successfully expressed and purified the photosensitive protein HeAR, examining its characteristics under both light and dark conditions. Transforming *E. coli* BL21(DE3) with a pET21c(+) plasmid containing the HeAR gene caused a color change from pale yellow to purple-red, confirming the purple hue of HeAR and its homolog BR. SDS-PAGE analysis indicated that both proteins have a molecular weight of approximately 27 kDa. Circular dichroism (CD) spectroscopy showed that HeAR's spectral features closely resemble BR's, with HeAR's maximum absorption wavelength red-shifted by 10 nm. This indicates a similar trimeric structure; however, there are subtle spectral differences that may be linked to environmental factors or variations in retinal isomer composition. Both HeAR and BR exhibited clear light-dark adaptation phenomena. In dark-adapted states, the

ratios of *HeAR*'s all-trans and 13-cis retinal isomers were 2:1 and 6:1, respectively, indicating a dynamic adjustment in retinal isomer composition in response to varying light conditions. Studies on photochemical reaction cycles showed that *HeAR*, similar to BR, undergoes a rapid cycle with L, M, and O intermediates when exposed to light. While the overall cycle time of *HeAR* is longer than that of BR, it exhibits faster M-state dynamics, indicating the presence of additional intermediates and greater reaction complexity. When illuminated, *HeAR* showed notable outward proton pumping activity, akin to BR. This proton pump mechanism allows *HeAR* to effectively transport H<sup>+</sup> ions from the cell interior to the exterior, achieving a hyperpolarization effect. In comparison to other photosensitive proteins, such as *NpHR* and *Archaerhodopsin-T*, *HeAR* has the potential for rapid neuronal inhibition even at low light levels. In conclusion, this study highlights the fundamental characteristics of *HeAR* and its similarities to BR, laying a theoretical groundwork for its future applications in neurobiology. As a novel photosensitive protein with unique photochemical properties and proton pump activity, *HeAR* could become a valuable tool in future optogenetic research.

**Author Contributions:** Writing—original draft preparation, visualization, L.C.; data analyses, writing—review and editing, project administration, Y.Y. All authors have read and agreed to the published version of the manuscript.

**Funding:** This research was funded by [Natural Science Foundation of Inner Mongolia Autonomous Region] grant number [2023LHMS03051 and 2019BS03005].

**Institutional Review Board Statement:** Not applicable.

**Informed Consent Statement:** Not applicable.

**Data Availability Statement:** Data are contained within the article.

**Conflicts of Interest:** The authors declare no conflict of interest.

## References

1. Seyedkarimi, M.S.; Aramvash, A.; Ramezani, R. High production of bacteriorhodopsin from wild type *Halobacterium salinarum*. *Extremophiles*. **2015**, *19*(5), 1021-1028.
2. Noji, T.; Ishikita, H. Mechanism of Absorption Wavelength Shift of Bacteriorhodopsin During Photocycle. *J Phys Chem B*. **2022**, *126*(48), 9945-9955.
3. Pan, Y.; Brown, L.; Konermann, L. Kinetic folding mechanism of an integral membrane protein examined by pulsed oxidative labeling and mass spectrometry. *J Mol Biol*. **2011**, *410*(1), 146-158.
4. Kawanabe, A.; Furutani, Y.; Jung, K.H.; Kandori, H. Engineering an inward proton transport from a bacterial sensor rhodopsin. *J Am Chem Soc*. **2009**, *131*(45), 16439-16444.
5. Kawatake, S.; Umegawa, Y.; Matsuoka, S.; Murata, M.; Sonoyama, M. Evaluation of diacylphospholipids as boundary lipids for bacteriorhodopsin from structural and functional aspects. *Biochim Biophys Acta*. **2016**, *1858*(9), 2106-2115.
6. Chen, Y.; Yeh, C.J.; Guo, Q.; Qi, Y.; Long, R.; Creton, C. Fast reversible isomerization of merocyanine as a tool to quantify stress history in elastomers. *Chem Sci*. **2020**, *12*(5), 1693-1701.
7. Johnson, T.J.; Gakhar, S.; Risbud, S.H.; Longo, M.L. Development and Characterization of Titanium Dioxide Gel with Encapsulated Bacteriorhodopsin for Hydrogen Production. *Langmuir*. **2018**, *34*(25), 7488-7496.
8. Zhang, Y.; Li, K.; Zang, M.; Cheng, Y.; Qi, H. Graphene-based photocatalysts for degradation of organic pollution. *Chemosphere*. **2023**, *341*, 140038.
9. Geldasa, F.T.; Kebede, M.A.; Shura, M.W.; Hone, F.G. Experimental and computational study of metal oxide nanoparticles for the photocatalytic degradation of organic pollutants: a review. *RSC Adv*. **2023**, *13*(27), 18404-18442.
10. Vasu, D.; Fu, Y.; Keyan, A.K.; Sakthinathan, S.; Chiu, T.W. Environmental Remediation of Toxic Organic Pollutants Using Visible-Light-Activated Cu/La/CeO<sub>2</sub>/GO Nanocomposites. *Materials (Basel)*. **2021**, *14*(20), 6143.
11. Ding, M.; Ao, W.; Xu, H. Facile construction of dual heterojunction CoO@TiO<sub>2</sub>/MXene hybrid with efficient and stable catalytic activity for phenol degradation with peroxy monosulfate under visible light irradiation. *J Hazard Mater*. **2021**, *42*, 126686.

12. Kawano, F.; Suzuki, H.; Furuya, A.; Sato, M. Engineered pairs of distinct photoswitches for optogenetic control of cellular proteins. *Nat Commun.* **2015**, *6*, 6256.
13. Repina, N.A.; Rosenbloom, A.; Mukherjee, A.; Schaffer, D.V.; Kane, R.S. At Light Speed: Advances in Optogenetic Systems for Regulating Cell Signaling and Behavior. *Annu Rev Chem Biomol Eng.* **2017**, *8*, 13-39.
14. Vlasova, A.D.; Bukhalovich, S.M.; Bagaeva, D.F. Intracellular microbial rhodopsin-based optogenetics to control metabolism and cell signaling. *Chem Soc Rev.* **2024**, *53*(7), 3327-3349.
15. Jeong, J.; Jung, J.; Jung, D. An implantable optogenetic stimulator wirelessly powered by flexible photovoltaics with near-infrared (NIR) light. *Biosens Bioelectron.* **2021**, *180*, 113139.
16. Vierock, J.; Rodriguez-Rozada, S.; Dieter, A. BiPOLES is an optogenetic tool developed for bidirectional dual-color control of neurons. *Nat Commun.* **2021**, *12*(1), 4527.
17. Amtul, Z.; Aziz, A.A. Microbial Proteins as Novel Industrial Biotechnology Hosts to Treat Epilepsy. *Mol Neurobiol.* **2017**, *54*(10), 8211-8224.
18. Ullrich, S.; Gueta, R.; Nagel, G. Degradation of channelopsin-2 in the absence of retinal and degradation resistance in certain mutants. *Biol Chem.* **2013**, *394*(2), 271-280.
19. Lemieux, C.; Otis, C.; Turmel, M. Ancestral chloroplast genome in *Mesostigma viride* reveals an early branch of green plant evolution. *Nature.* **2000**, *403*(6770), 649-652.
20. Zhang, F.; Prigge, M.; Beyrière, F. Red-shifted optogenetic excitation: a tool for fast neural control derived from *Volvox carteri*. *Nat Neurosci.* **2008**, *11*(6), 631-633.
21. DuBois, D.W.; Murchison, D.A.; Mahnke, A.H. Maintenance of optogenetic channel rhodopsin (ChR2) function in aging mice: Implications for pharmacological studies of inhibitory synaptic transmission, quantal content, and calcium homeostasis. *Neuropharmacology.* **2023**, *238*, 109651.
22. Okhrimenko, I.S.; Kovalev, K.; Petrovskaya, L.E. Mirror proteorhodopsins. *Commun Chem.* **2023**, *6*(1), 88.
23. Trachtová, S.; Spanová, A.; Horák, D.; Kozáková, H.; Rittich, B. Real-Time Polymerase Chain Reaction as a Tool for Evaluation of Magnetic Poly(Glycidyl methacrylate)-Based Microspheres in Molecular Diagnostics. *Curr Pharm Des.* **2016**, *22*(5), 639-646.
24. Yamada, M.; Okada, Y.; Yoshida, T.; Nagasawa, T. Vanillin production using *Escherichia coli* cells over-expressing isoeugenol monooxygenase of *Pseudomonas putida*. *Biotechnol Lett.* **2008**, *30*(4), 665-670.
25. Cubizolle, A.; Cia, D.; Moine, E. Isopropyl-phloroglucinol-DHA protects outer retinal cells against lethal dose of all-trans-retinal. *J Cell Mol Med.* **2020**, *24*(9), 5057-5069.
26. Zhang, X.; Miller, K.W. Dodecyl maltopyranoside enabled purification of active human GABA type A receptors for deep and direct proteomic sequencing. *Mol Cell Proteomics.* **2015**, *14*(3), 724-738.
27. Wang, X.; Long, H.; Shen, D.; Liu, L. Cloning, expression, and characterization of a novel sialidase from *Brevibacterium casei*. *Biotechnol Appl Biochem.* **2017**, *64*(2), 195-200.
28. Goyon, A.; McDonald, D.; Fekete, S.; Guillarme, D.; Stella, C. Development of an innovative salt-mediated pH gradient cation exchange chromatography method for the characterization of therapeutic antibodies. *J Chromatogr B Analyt Technol Biomed Life Sci.* **2020**, *1160*, 122379.
29. Dai, G.; Geng, X.; Chaoluomeng. Photocycle of sensory rhodopsin II from *Halobacterium salinarum* (HsSRII): Mutation of D103 accelerates M decay and changes the decay pathway of a 13-cis O-like species. *Photochemistry and Photobiology*, **2018**, *94*(4), 705-714.
30. Chen, Z.; Tang, M.; Wang, Z. The Effects of Q-Switched Nd:YAG Laser Irradiation in the Wavelength of 1064nm and 532nm on Guinea Pigs' Skin Tissue. *Conf Proc IEEE Eng Med Biol Soc.* **2005**, *2005*, 6809-6812.
31. Lee, H.W.; Park, J.H.; Kim, W.K. Engineered *Escherichia coli* strains as platforms for biological production of isoprene. *FEBS Open Bio.* **2020**, *10*(5), 780-788.
32. Maeda, A.; Iwasa, T.; Yoshizawa, T. Isomeric composition of retinal chromophore in dark-adapted bacteriorhodopsin. *Journal of Biochemistry*, **1977**, *82*(6), 1599-1604.

33. Awasthi, M.; Ranjan, P.; Sharma, K.; Veetil, S.K.; Kateriya, S. The trafficking of bacterial type rhodopsins into the Chlamydomonas eyespot and flagella is IFT mediated. *Sci Rep.* 2016, 6, 34646.
34. Tóth-Boconádi, R.; Taneva, S.G.; Keszthelyi, L. Actinic light-energy dependence of proton release from bacteriorhodopsin. *Biophys J.* 2005, 89(4), 2605-2609.

**Disclaimer/Publisher's Note:** The statements, opinions and data contained in all publications are solely those of the individual author(s) and contributor(s) and not of MDPI and/or the editor(s). MDPI and/or the editor(s) disclaim responsibility for any injury to people or property resulting from any ideas, methods, instructions or products referred to in the content.